

Supporting Information

Self-Decomposable Mesoporous Doxorubicin@Silica  
Nanocomposites for Nuclear Targeted  
Chemo-Photodynamic Combination Therapy

*Jie Wang,<sup>†</sup> Dajun Xu,<sup>†</sup> Tao Deng,<sup>†</sup> Yunyan Li,<sup>†</sup> Le Xue,<sup>†</sup> Tong Yan,<sup>‡</sup> Dechun*

*Huang,<sup>\*†</sup> and Dawei Deng<sup>\*†,‡</sup>*

<sup>†</sup> Department of Pharmaceutical Engineering and <sup>‡</sup> Department of Biomedical Engineering, School of Engineering, China Pharmaceutical University, Nanjing 210009, P. R. China.

\* Corresponding author. Email: dengdawei@cpu.edu.cn or cpuhdc@cpu.edu.cn

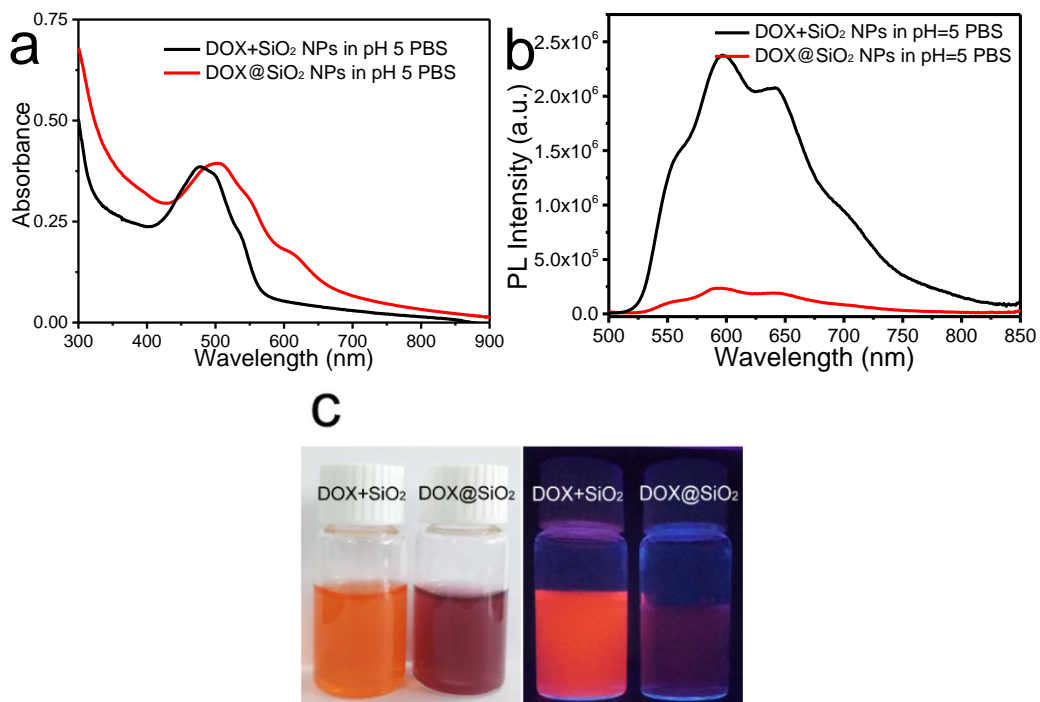


Fig. S1 (a) Absorption and (b) PL spectra of DOX@SiO<sub>2</sub> NPs and pure SiO<sub>2</sub> NPs mixed with DOX in pH 5 PBS. (c) Photographs of pure SiO<sub>2</sub> NPs mixed with DOX and DOX@SiO<sub>2</sub> NPs in pH 5 PBS taken under room light (left) and 365 nm UV light (right).

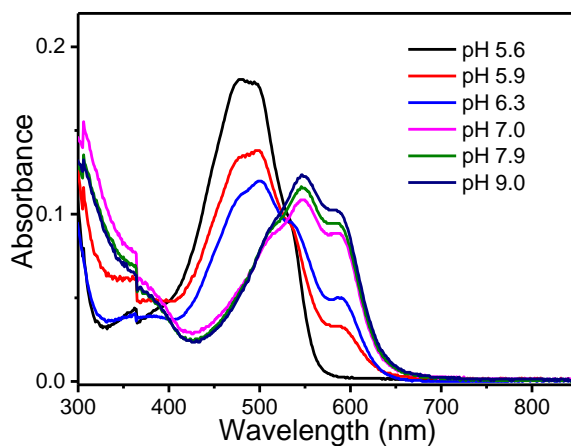


Fig. S2 Absorption spectra of aqueous DOX solution at different pH. The solution pH was adjusted by adding 0.05 M NaOH.

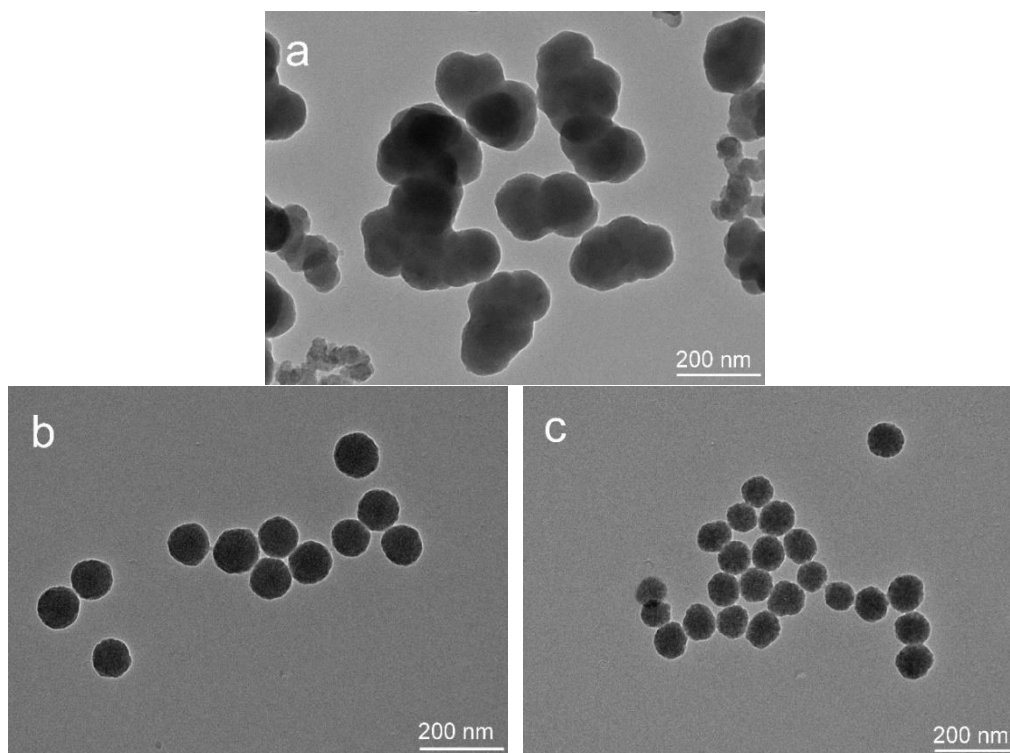


Fig. S3 TEM images of DOX@SiO<sub>2</sub> NPs prepared at different initial pH: a, 9.5; b, 8.5; c: 8. The pH in the reaction media was tuned by varying the amount of aqueous ammonia.

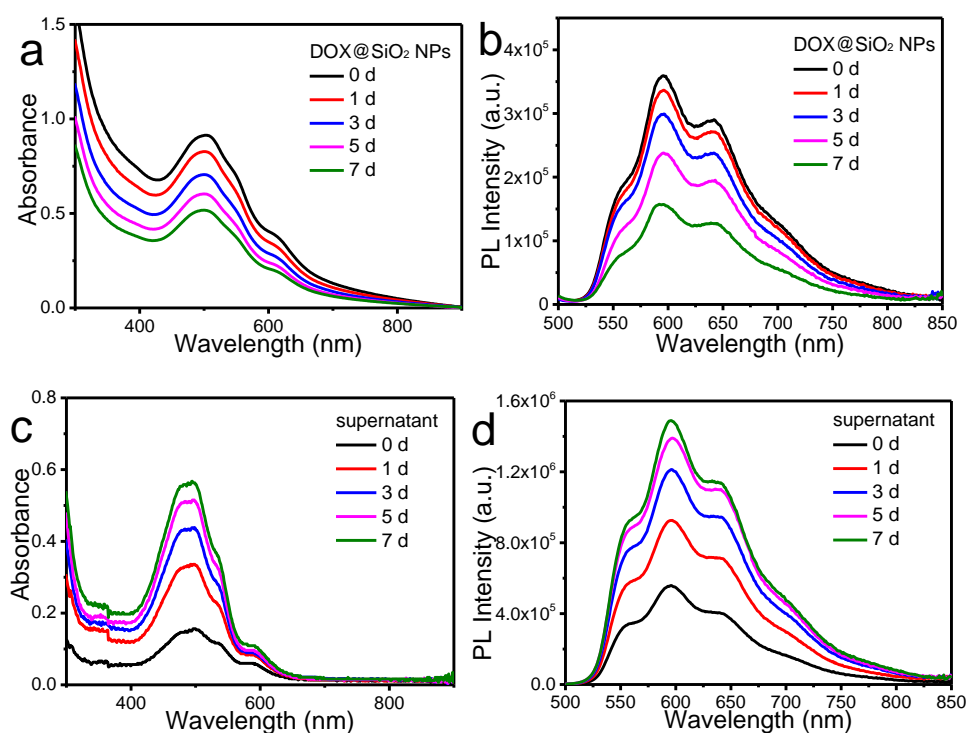


Fig. S4 (a) Absorption and (b) PL spectra of DOX@SiO<sub>2</sub> NPs separated via centrifugation after incubated in pH=5 PBS for different periods of time. (c) Absorption and (d) PL spectra of the corresponding supernatant.

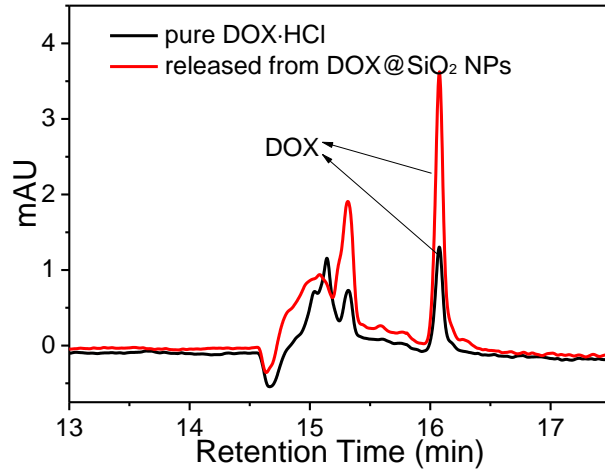


Fig. S5 High performance liquid chromatography results of pure DOX·HCl dissolved in deionized water, and the supernatant obtained from DOX@SiO<sub>2</sub> NPs after incubated in pH 5 PBS.

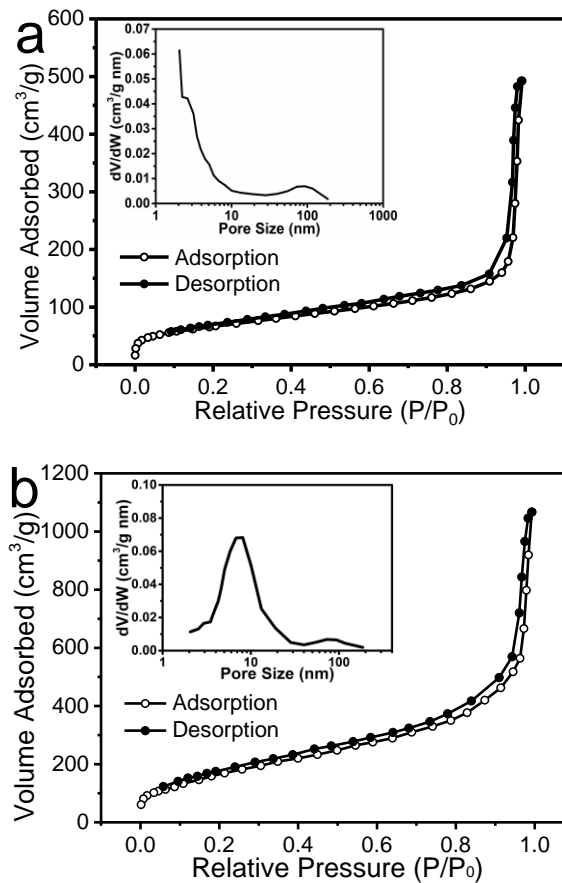


Fig. S6 Nitrogen adsorption-desorption isotherms and Barrett-Joyner-Halenda pore size distributions (insets) of mDOX@SiO<sub>2</sub> NPs (a) before and (b) after incubated in pH 5 PBS for 3 d.

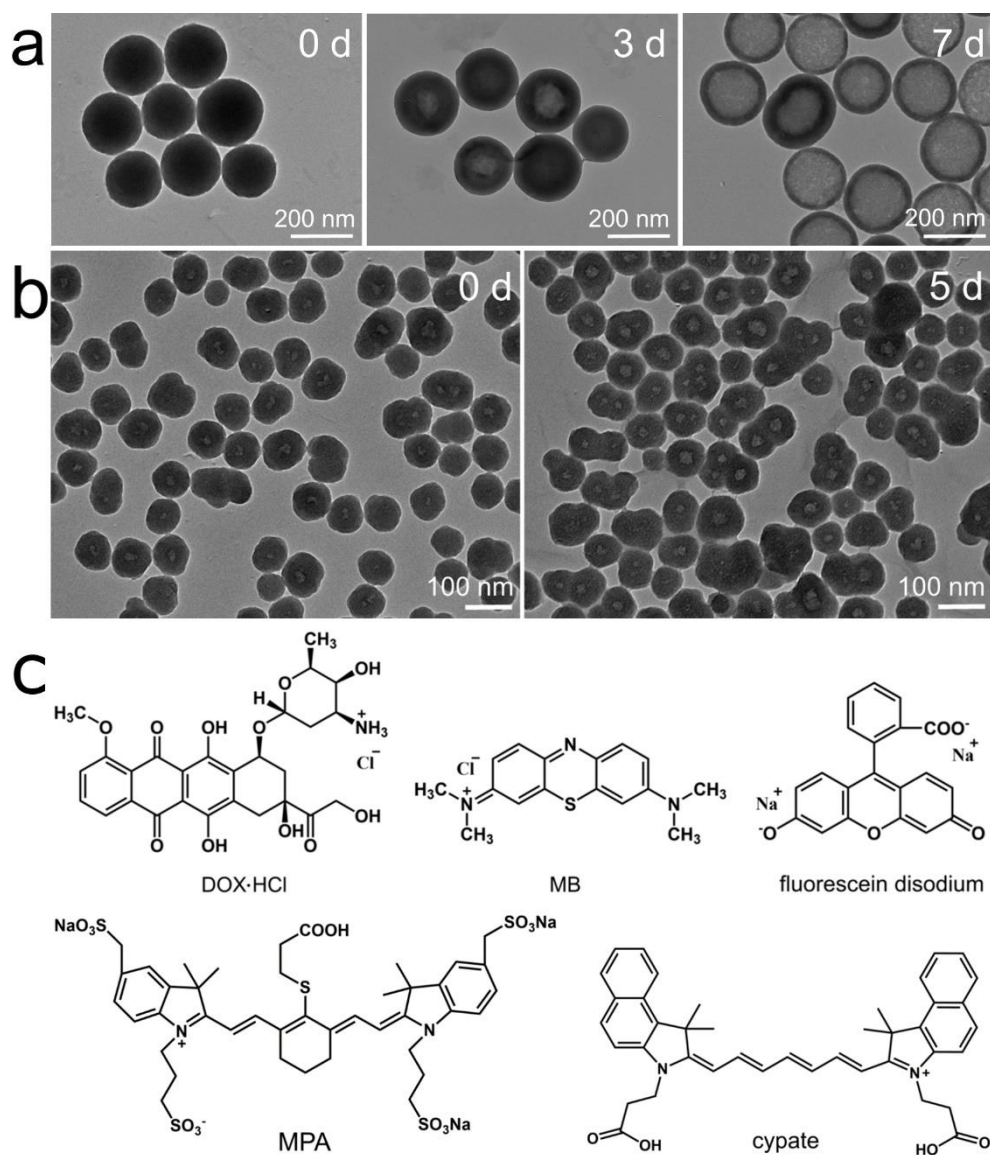


Fig. S7 Representative TEM images of (a) MB-embedded SiO<sub>2</sub> NPs and (b) fluorescein-embedded SiO<sub>2</sub> NPs after incubated in deionized water for different periods of time. (c) Chemical structures of DOX·HCl, MB, fluorescein disodium, MPA (NIR fluorescent dye) and cypate (NIR fluorescent dye).

From Fig. S7a, the center-first decomposition of MB-embedded SiO<sub>2</sub> NPs was clearly observed and found to be intrinsic (regardless of particle size or MB concentration). It was proposed that the electrostatic attraction between positively charged MB and negatively charged silica species (product of TEOS hydrolysis), and the high MB concentration at the beginning of NP growth, would result in MB-rich nucleus and lead to center-first decomposition via a diffusion controlled MB release.<sup>1</sup> Accordingly, we selected fluorescein that should be negatively charged in the basic reaction media to prepare fluorescein-embedded SiO<sub>2</sub> NPs. Interestingly, similar center-first decomposition pattern was observed (Figure S7b). Moreover, two indocyanine green derivative near-infrared (NIR) fluorescent dyes (Figure S7c) were found difficult to be embedded into SiO<sub>2</sub> NPs. These

results suggest that (i) the slightly negative charge of DOX in reaction media should not be the main contribution to the formation of mDOX@SiO<sub>2</sub> NPs, and (ii) molecular size of drug molecules might affect decomposition behavior. Larger molecular size of DOX than MB or fluorescein may account for the formation of mDOX@SiO<sub>2</sub> NPs (Figure S7c). During NP growth, once a DOX molecule was incorporated, the relatively larger size would radially inhibit further cross-linking of silica species, leading to a less homogeneous concentric distribution of DOX molecules. Nevertheless, other factors such as molecule conformation and interaction between specific functional groups may also play important roles, making it hard to generalize a specific decomposition manner to a category of drug molecules.

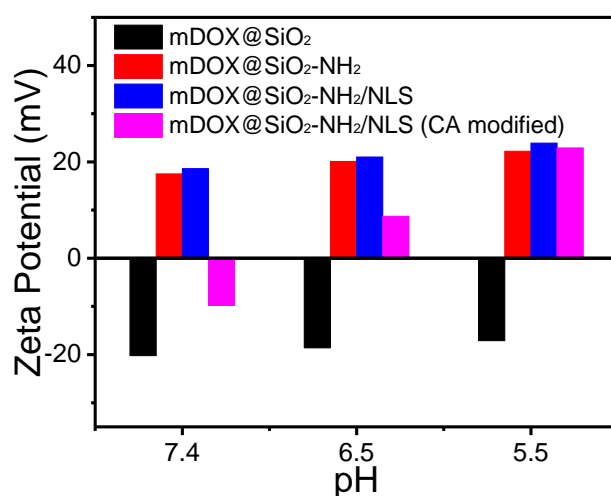


Fig. S8 Zeta potential of the mDOX@SiO<sub>2</sub> NPs after different modifications in PBS of different pH.

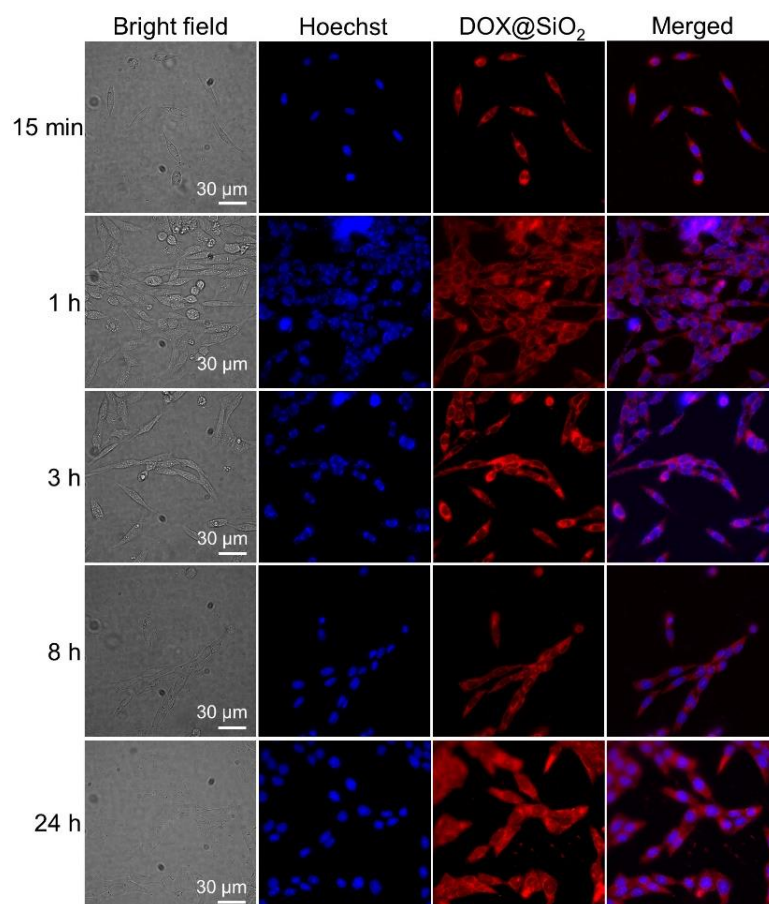


Fig. S9 Representative LCSM images of U87MG cells after co-incubated with DOX@SiO<sub>2</sub> NPs for different time. The stronger nuclear distribution at 24 h was ascribed to the release of DOX molecules.

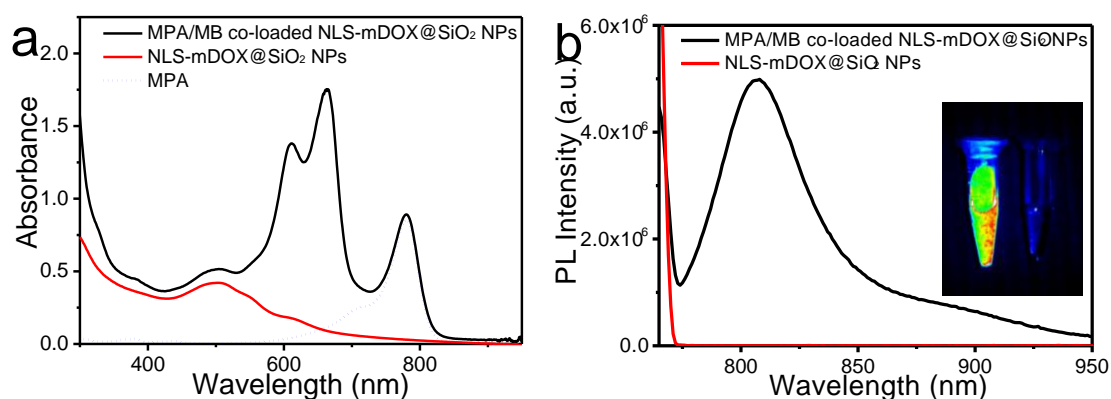


Fig. S10 (a) Absorption spectra of MPA/MB co-loaded NLS-mDOX@SiO<sub>2</sub> NPs, NLS-mDOX@SiO<sub>2</sub> NPs and MPA. The original MPA/MB weight ratio used for uploading was about 5/1. (b) PL spectra of MPA/MB co-loaded NLS-mDOX@SiO<sub>2</sub> NPs and NLS-mDOX@SiO<sub>2</sub>.  $\lambda_{ex}=765$  nm. The inset shows the pseudocolored image of the two sample (left) with or (right) without MPA loading.

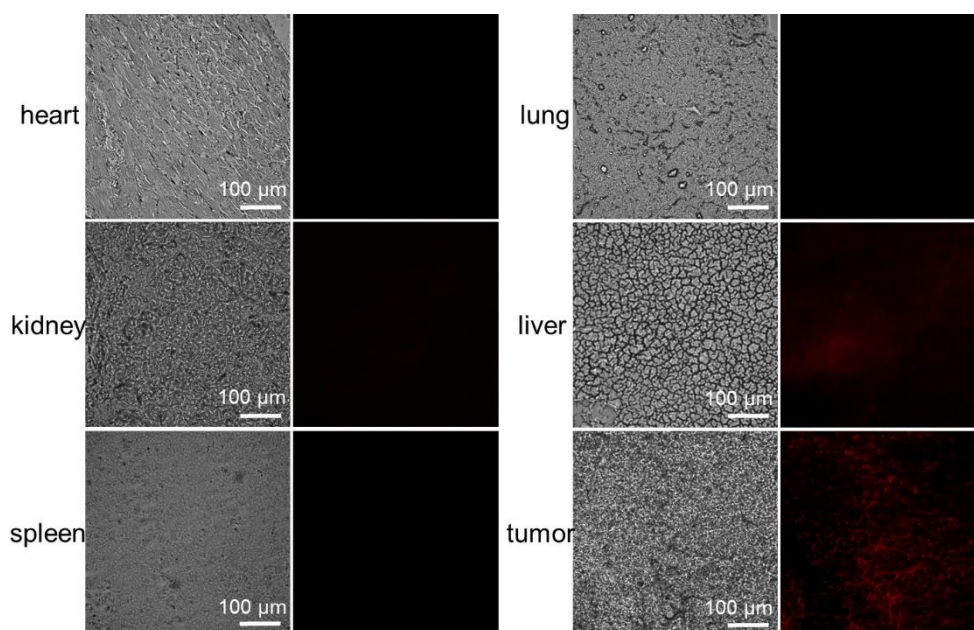


Fig. S11 Representative fluorescence images of organ slices from mice. The mice were treated with MPA/MB co-loaded NLS-mDOX@SiO<sub>2</sub> NPs and were sacrificed 24 h post injection.

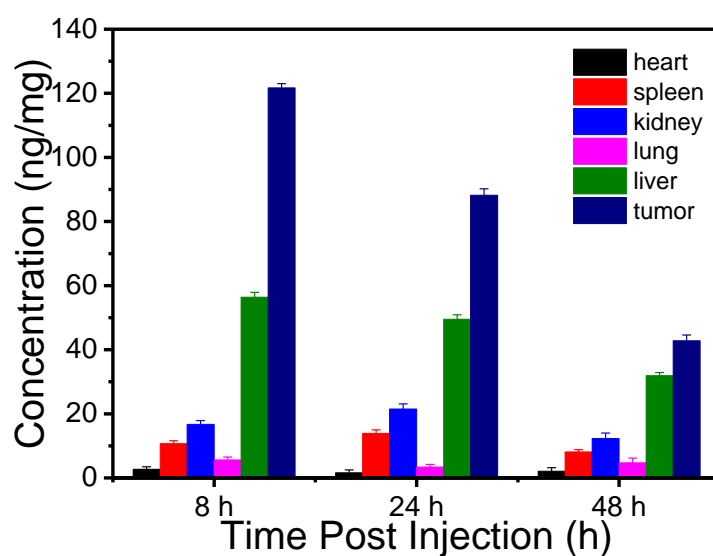


Fig. S12 ICP-MS-determined Si biodistribution in U87MG tumor-bearing mice after treated with NLS-mDOX@SiO<sub>2</sub> NPs for different times.

#### References

- (1) Zhang, S.; Chu, Z.; Yin, C.; Zhang, C.; Lin, G.; Li, Q. Controllable Drug Release and Simultaneously Carrier Decomposition of SiO<sub>2</sub>-Drug Composite Nanoparticles. *J. Am. Chem. Soc.* **2013**, *135*, 5709–5716.